FAILURE ANALYSIS OF THE ARECIBO OBSERVATORY M4N AUXILIARY CABLE[1]

Gregory J. Harrigan,[2] Vinay K. Goyal,[3] Pavel F. Babuska,[4] Nathan Trepal[5]

ABSTRACT: Structural and forensic analysis concluded that the Arecibo Observatory M4N socket joint failure in August 2020 was due to a socket joint design with insufficient design criteria that did not explicitly consider socket constituent stress margins or time-dependent damage mechanisms. The socket attachment design was found to have an initially low structural margin with a finite service life, notably in the outer socket wires, which degraded primarily due to long-term zinc creep effects that were activated by long-term sustained loading and exacerbated by cyclic loading. Additionally, HAC and wire defects were found in a few outer wires that may also have contributed to initial outer wire failures. The design did not explicitly consider the time-dependent effects of creep and cyclic loading on design capability, account for a worst-case build condition traceable to in-service inspection of features (e.g., zinc creep/extrusion), specify an end-of-life capability requirement associated with service life degradation, or explicitly set service life inspection intervals with pass/fail inspection criteria. In-service inspections showed evidence of progressive zinc extrusion on several Arecibo sockets, which in hindsight were evidence of cumulative damage and effectively a missed opportunity to prevent cable failure. Open spelter sockets of this type are used throughout industry in stay cables. Recommendations are proposed to prevent failures of similar socket joints, including verification of positive stress margins in socket joint wires for all failure modes, periodic visual inspections with acceptance criteria for zinc extrusion that are tied to structural qualification, and revisiting codes and industry standards based on lessons learned from this analysis.

Keywords: Arecibo Observatory, collapse, creep, fatigue, socket

ANÁLISIS DE FALLO DEL CABLE AUXILIAR DEL OBSERVATORIO DE ARECIBO

RESUMEN: Se llevaron a cabo análisis estructurales e investigaciones forenses que concluyeron que la falla del cable auxiliar del Observatorio de Arecibo en agosto del 2020 fue por causa de un diseño insuficiente que no consideró los márgenes de seguridad estructurales del cable o los mecanismos de daño que pueden ocurrir cuando una carga sostenida actúa en un cable por un tiempo largo. Se encontró que el diseño de la conexión del enchufe tenía un margen de seguridad inicialmente bajo, en particular en los cables del enchufe exterior, que se degradaba principalmente por la deformación excesiva del zinc que ocurrió a causa de la carga sostenida y que se agravó por la carga cíclica. Además, se encontraron defectos en algunos cables externos que también pudieron haber contribuido a las fallas iniciales de estos cables. El diseño inicial no se establecieron los intervalos de inspección de la vida útil con criterios de inspección para reparaciones. La verificación no consideró casos extremos donde la construcción del cable no fue óptima. Las inspecciones de servicio mostraron evidencia de extrusión progresiva del zinc en varios enchufes del observatorio, que en retrospectiva eran evidencia de daño acumulativo y, en efecto, una oportunidad perdida para prevenir la falla del cable. Los enchufes de este tipo se utilizan en toda la industria. Se proponen las siguientes recomendaciones para prevenir fallas de juntas de enchufe similares: (1) Deben verificarse los márgenes estructurales de tensión en todos los cables, (2) Deben implementarse inspecciones visuales

periódicas ligadas a la calificación estructural con un criterio de aceptación para la extrusión del zinc en el enchufe, (3) Deben revisarse los códigos civiles y estándares de la industria a base de las lecciones aprendidas en esta investigación.

Palabras clave: Observatorio de Arecibo, cable auxiliar, diseño de enchufes estructurales, colapso, fatiga

INTRODUCTION

The Arecibo Observatory is a radio astronomy, solar system radar, and atmospheric physics facility that was constructed in 1963 and periodically upgraded. In the 1990s, the structure underwent a major upgrade to include auxiliary main cables and extra backstay cables to increase the capability of the feed platform to support a much larger instrument and suspended platform structure called the Gregorian Dome. The observatory structural elements consist of three towers spaced 120 degrees apart that supported main, auxiliary, and backstay cables to keep the receiver platform and instrument supported and controlled with extreme precision. After the upgrades in the 1990s, each tower received another pair of 3.25-inch auxiliary main cables and two additional 3.625-inch backstay cables to support the upgraded mass. An open spelter socket termination was used on the tower end of the cable, while slightly different termination types were used on the feed platform side.

Sequence of Failure Events: First Cable Failure to Observatory Collapse

In the middle of the night on August 10, 2020, an auxiliary main cable (denoted Aux M4N) failed and pulled free from the North side of Tower 4 during normal observatory operations. On November 6, 2020, one of the four original main cables of Tower 4 failed. This second cable failure differed from the Aux M4N failure in that it was one of the original main cables, which employed a different structural strand construction and a different cable termination type. On December 1, 2020, a second original main cable failed, causing a chain reaction of failures and load imbalances in the observatory suspension cable system that led to the total collapse of the observatory and supporting tower segments. A previous investigation reflected upon the collapse of the Observatory, Reference 1.
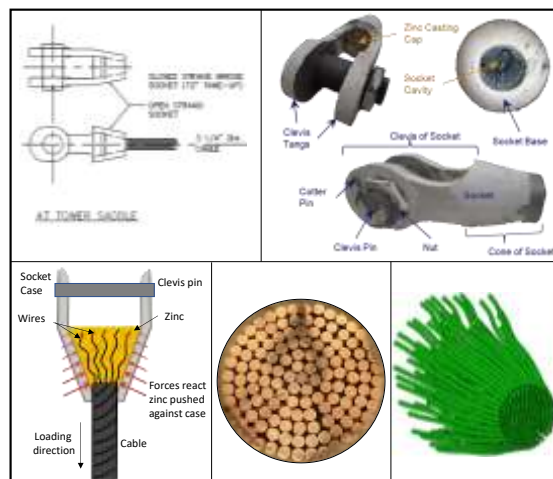
Figure 1: Clockwise starting on the top left: Open spelter socket drawing, socket terminology, Aux M4N broomed wire reconstruction, 1 × 127 structural strand cross section, and cable-socket interface detail sketch.

Overview of the Cable - Open Spelter Socket Joint

This failure analysis focused on the Aux M4N cable failure, which was manufactured by Wirerope Works, Inc. (Reference 2) in 1993, since it instigated the chain of events leading to the collapse of the Observatory. The cable failed near the joint where the cable connects with the open spelter socket, Figure 1. Specifically, the Aux M4N structural strand follows a 1×127 construction and consists of 126 individual 0.25-inch diameter wires wrapped around a single, seven-wire strand in six concentric rings with a pattern of 6, 12, 18, 24, 30, 36 wires. Zinc spelter socket joints are terminations in stay cables used throughout industry that transfer loads between adjacent structures. Terminations consist of stay cable wires that are unraveled, broomed, and then embedded/bonded into a zinc casting inside a conical volume. Cable tension wedges the zinc material against the slanted conical surface, which then develops a large compression zone within the zinc such that if a failure were to occur it is expected to be outside the socket joint in the cable span. This type of open spelter socket joint is extensively used in structural applications because it is highly efficient and reliable.

Cable tensions from observatory dead load, operational loads, and survival transients are transmitted to the socket termination through the 126 individually broomed wires that are held in place by the cast zinc spelter within the steel open socket conical volume, Figure 1. The zinc that fills the socket cavity is bonded to the wires, and this bond creates an efficient load transfer among the wires within the socket. A special characteristic of the socket termination is that the combination of zinc plasticity and the conical volume forces a "squeezing" effect to occur around the broomed wire bundle in the narrow part of the socket. The high confining pressures experienced at the outlet of the socket keep the broomed wires from pulling out of the zinc and allow the failure to occur in the cable outside the socket, thus developing the cited 100% efficiency termination. These physics were confirmed using finite element (FE) models.

Table 1: Major categories of the fishbone failure diagram.

1. Design	2. Loads/Environments	3. Build Variability
a. Insufficient Design Criteria	a. Improper Nominal Loads Characterization	a. Zinc Spelter
b. Material Incompatibility	b. Improper Survival Loads Characterization	b. Wires
c. Insufficient Qualification	c. Improper Moisture Environment Characterization	c. Wire Brooming
d. Insufficient Acceptance Criteria		d. Socket Casing
e. Insufficient Inspection Criteria		e. Poor Wire/Zinc Bond
4. Environmental Assisted Degradation	**5. Failure Mechanisms**	
a. Corrosion	a. Fatigue	
b. Hydrogen-assisted Cracking	b. Creep	
c. Stress Corrosion Cracking	c. Strength	

FORENSIC AND STRUCTURAL FAILURE ANALYSIS

A best-effort systematic fishbone was developed to evaluate supporting and refuting evidence for each potential causal factor of the M4N Auxiliary Main cable (Reference 3). Cause and effect hypotheses were developed for each factor and evaluated for credibility using supporting/refuting evidence. Rating criteria used by the team assigned a credibility rating and a contribution level based on a weighing of evidence. The credibility rating and a severity of contribution were used to rank potential factors and develop credible

failure scenarios. A scenario matrix was developed from the fishbone dispositions and prioritized based on the credibility rating (see Table 1). This matrix was used to develop a likely progression of failure and most probable contributing factors and considered the following factors: (1) Design, (2) Loads and Environments, (3) Build Variability, (4) Environmental Assisted Degradation, and (5) Failure Mechanisms.

Forensic Failure Analysis

A forensic analysis for the Aux M4N socket, clevis pin, and cable end was conducted in collaboration with Wiss, Janney, Elstner Associates, Inc. (WJE). Evidence was protected from further degradation to the extent feasible while at Arecibo and through transportation to Kennedy Space Center (KSC) for further laboratory analysis. The activities included visual inspection and chemical analysis, followed by nondestructive analysis, which included radiography and magnetic particle inspections, metrology, and three-dimensional (3D) laser scanning. 3D laser scanning was performed prior to sectioning and after each sectioning step to improve the surface topography captured from within the socket. 3D prints were made as forensic support aids from the 3D laser scans. Visual examination revealed that the ultimate separation of the cable connection occurred via fracture of some of the wires within the socket cone and the zinc casting itself.

The socket was dissected, first longitudinally into left and right halves, followed by transverse cuts in each half starting from the casting cap side of the socket halves and moving toward the wire fractures near the socket base, Figure 2. During the sectioning process, areas of interest were analyzed and/or sectioned off for further microscopy. The zinc casting was analyzed by metallography, and the wire fractures were extracted from the zinc for fractography. Lastly, material testing was performed on socket and virgin material to characterize mechanical and metallurgical properties.

The wire fracture surfaces embedded in the socket zinc casting were in various states of accessibility, with some protruding from the casting, some observed along the concave surfaces of the casting inner diameter, and others completely buried in zinc and not visible (where the transverse band saw cut revealed the presence of these wires within the zinc casting volume). Initially, wire fracture surface removal was attempted by mechanical means. Abrasive cutoff wheels were used to cut the slices into smaller, more manageable pieces to access the individual fractured wire ends during dissection, and to cut samples for scanning electron microscopy (SEM), mechanical testing, and metallography. Fractography analysis of the wires required removal of the zinc surrounding the wires to expose any fracture surfaces encased by the zinc because of the overall socket failure. To expose the fracture surfaces of wires for analysis, the zinc was removed via dissolution in hydrochloric acid, Figure 2. Additional sectioning of casting was performed to examine features and create test coupons for mechanical properties testing.

Figure 2: Sectioning plan for the socket (top left), sectioned zinc (top right), section of zinc with encased wires before (bottom left) and after (bottom right) removal of zinc via dissolution in acid.

Structural Failure Analysis

High-fidelity three-dimensional FE models of the cable termination into the M4N socket were developed using Abaqus to investigate the individual wire, zinc, and steel socket mechanics and to support the failure investigation. The models enabled sensitivity studies to understand the effects of various parameters including the degree of wire brooming, zinc material properties, and metallurgic examinations. Multiple model configurations were constructed, each containing varying levels of wire brooming, one of which represented the as-built/as-failed wire brooming specific to Aux M4N. The interfaces between the wires and zinc were modeled with a nearly infinite stiffness contact condition to enable extracting interface shear and pressure stresses. Contact modeling with friction was implemented between the zinc and the socket casing to allow for zinc "seating" within the socket. Material nonlinearity was included for the steel wires and the zinc spelter to predict the post-yield material response. Examples of the idealized wire brooming, simplified socket model, and wedge model mesh density are shown in Figure 3.

True stress-strain curves were generated and incorporated into the models based on NASA testing of the steel wire and the zinc. Stress-strain curves for the various material systems were approximated using the Ramberg-Osgood method. Pure zinc in structural socket terminations has low tension and high compression strengths, and grain sizes vary based on manufactured method and rates of cooling during casting. A high-confidence material model that accurately reflects both tension and compression response or attempts to model progressive damage is challenging. Zinc properties from material testing also exhibited significant dispersions. Different zinc nonlinear models were used in sensitivity studies to predict socket termination capability to address the uncertainty in the zinc mechanical behavior.

.

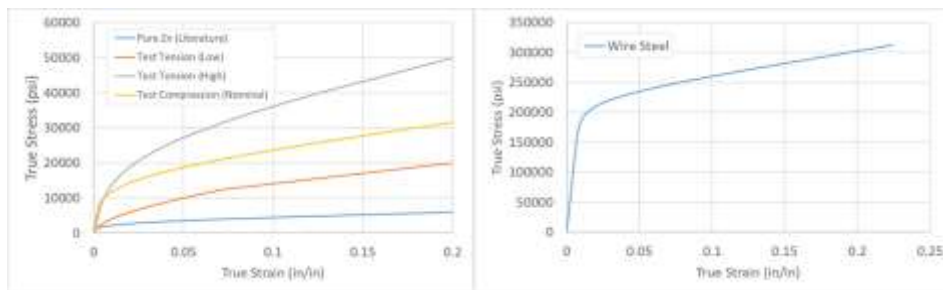**Figure 3: FE model included conical socket housing, cast zinc, and individual wires.**

Figure 4:. True sStress-sStrain cCurves for the rRange of zZinc mMaterial pProperties (left) and bBaseline sSteel mMaterial pProperty (right).

FAILURE ANALYSIS RESULTS

Forensic and structural analysis were performed to assess the credibility of fishbones presented in Table 1.

Loads and Environments in Service

Improper Nominal Loads: The first load experienced by a newly manufactured socket is the socket proof test to 50% of the specified cable breaking strength. In the case of Aux M4N, this corresponds to a load of 657 kips, given the catalog rated breaking strength of 1314 kips. Regarding operational loads, the observatory drawings specified three relevant loading cable conditions for the Aux Main cable: (1) Condition 1: Initial tension under dead loads at 90 degrees F and includes all loads from modified central feed structure, the new Gregorian Dome, cables, loads due to raising the platform, loads due to tie-downs, and loads from wave guide supporting system. The final loads after initial erection is 602 kips. (2) Condition 2: Operational loads include all loads in Condition 1 plus 50-mph wind and 90 degrees F: 615 kips. (3) Condition 3: Operational loads include all loads in Condition 1 plus 100-mph wind and 90 degrees F: 622 kips.

WJE performed structural loads analysis and found that cable loads were affected by routine movement of the telescope and by wind loading during "survival" events. During routine operation, the movements cause loading imbalances in the cable suspension structure, while the tie-downs counter the imbalance so the auxiliary cable tensions vary only by the proportion of the additional tie-down force and auxiliary cable angles. WJE generated envelope values for each cable in this process. During "survival" conditions, the

Gregorian Dome is stowed, and tie-down forces are relaxed so that the observatory receiver is free to displace as needed with the winds. WJE's analysis predicted a maximum cable load of 720 kips (Reference 4), nearly 100 kips higher than the value prescribed in the drawing. Dead loads were a significant portion of the maximum cable load: (602 kips/720 kips) ~84% resulting in a design factor of safety against the 1314-kip cable breaking strength of approximately (1314 kips/720 kips) ~1.83. Finally, a proof factor of roughly 0.92 is achieved when considering a proof test of 657 kips and a survival load of 720 kips. The higher loads predicted by WJE exceeded those specified in the drawing and resulted in a lower factor of safety (1.83) and lower proof factor compared with design intent.

Improper Survival Loads: Fluctuating cable loads and corresponding load spectra due to wind oscillations from hurricanes, earthquakes, temperature fluctuations, and telescope movements was not fully characterized. When examining the three loading conditions per the drawings, loads caused by winds are a small percentage of the total cable loads based on a comparison of Load Conditions 1, 2, and 3. Strain-gage and load cell data collected over a multi-day window demonstrated that typical wind and temperature fluctuations produced small cable loads in comparison with the sustained loads from dead weight of the various Arecibo radio telescope structures. Analysis of this factor focused on whether improperly characterized survival loads (e.g., earthquake, hurricane, extreme temperatures) caused the hardware to be used beyond its design capability. The real structural response due to wind gusts or vortex shedding during transient environments such as hurricanes is unknown and can only be qualitatively assessed as a general contributor to the accumulation of damage occurring in the socket joint. Given the high percentage of deadload compared to the total load in the cable (~84%), failure of the socket joint is largely due to accumulation of damage due to creep and accelerated by cyclic loading. The Aux M4N cable failure occurred on a day with benign wind/thermal environments and without operation of the observatory receiver. Due to the significant dead loads compared with transient loads in this design, improper characterization of survival loads was deemed a low but still notable factor in the failure event.

Improper Moisture Characterization: Failure analysis showed pervasive corrosion associated with moisture within the socket joint. Structural qualification of the cable was for a pristine configuration rather than being derated for decades of moisture exposure, corrosion, and weather events. Actions were taken over the service life to prevent observed water intrusion, indicating conditions were not adequately considered during the design process. Despite these observations, excised wire segments were found to be in-family with nominal strengths. The conclusions on corrosion within the zinc as a contributor are discussed later.

Design

Insufficient Design Criteria: FE analyses predicted significant yielding of outer wires and negative structural margins using the maximum predicted cable loads of 720 kips predicted by WJE. Even using an applied load of 600 kips, outer wire stress predictions were in the 220 - 230 ksi range based on a range of zinc material models. With a factor of safety of unity, this corresponded to structural margins ranging from +15% to –4% when considering a range of wire ultimate strengths of 220 to 250 ksi. In aerospace applications, structures are analyzed and compared not only against the breaking strength of the joint but also for constituent stresses against their respective material strengths.
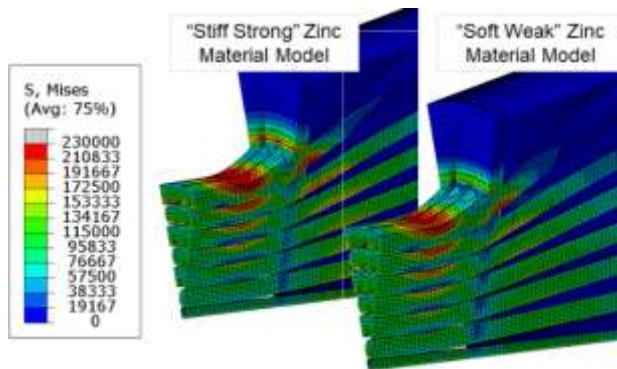
Figure 5:- Outer wire stresses were near capacity regardless of zinc material model at design loads.

Based on loads alone, the effective design factor of safety was calculated as 1.83, which is lower than typical industry standards. The design upgrades involving the failed socket joint predated ASCE 19-96 (Reference 5), which was the requirements document governing the design of steel cables for buildings. ASCE 19-96 was superseded by ASCE 19-10 (Reference 6). While the inapplicability of ASCE 19-10 to the failed socket design is recognized, it was found that the effective design factor in this application fell short of the 2.2 specified in that standard and even those specified in international standards (Reference 7). The ASCE standard also states the minimum breaking strength of cables shall always be at least twice the maximum cable design loads, including the envelope of loading combinations of cable self-weight, structure dead load, cable pre-stress forces, and live load and environmental load combinations. Consequently, given the negative structural margins and insufficient factor of safety, insufficient design criterion was identified as significant contributor to the failure event.

Insufficient Acceptance Criteria and Inspections: While the drawing did not specify acceptance criteria or characteristics for wire brooming, forensic reconstruction of the brooming (Figure 1) was found to be in-family to other socket builds. Nondestructive evaluation of the socket joint was not performed prior to service, but forensic examination of the failed socket showed dimensions to be within specifications. Defects (e.g., voids/cracks) within the zinc such as gas bubbles toward the socket back side were found (Figure 6), but analytical models with representative void geometries predicted negligible effects on the outer wire stresses near the termination. This is because the most highly stressed wires occur near the socket base and remain unaffected by the existence of voids a substantial distance away in the zinc. Further, a separate model simulated the existence of a cavity tear near the casting cap, but no changes in critical wire stress levels resulted as termination capacity is influenced significantly by the zinc in the narrow side of the conical volume but is largely unaffected by the zinc at the open end of the socket.

Inspection limitations prevent the ability to characterize defects within the zinc casting of a particular build, thus preventing the qualification test from accounting for worst-case build conditions without some other destructive process. Inspection criteria were not traceable to the qualification program, despite easily observable and measurable zinc extrusion at the socket joint base. In-service inspections conducted over the socket life showed evidence of zinc extrusion and moisture intrusion/corrosion. Records and socket

failure analysis showed that corrosion mitigations were employed, and that the zinc extruded progressively between 2003 (0.5 inch) and 2019 (1 3/8 inches). Although no pass/fail criteria were known to exist, AASHTO M277-06 states that seating extrusion should be less than one-sixth of the cable diameter, or less than 0.6 inch for the Auxiliary M4N cable that failed (Figure 6). The inspection process did not couple the qualification/design process to a pass/fail criterion to trigger a replacement.

Figure 6. Close-up view of a single gas bubble in zinc casting (left); 2003 photo of aAux M4N (left) showing ~0.5-inch zZinc sSeating eExtrusion (middle); and 2019 pPhoto (right) showing ~1 3/8-inches Extrusion. (Ref. 4)

Build Variability

Wires: Independent mechanical testing of excised/recovered wire material from the Aux M4N socket showed conforming dimensions and mechanical properties. Failure analysis of the socket verified that the cross section met drawing and had the correct number of wires. At least two wires had surface defects (Figure 7) that likely contributed to wire fractures. The negative structural margins in the outer wires likely deteriorated further for those wires with surface defects, as these act as stress risers.

Socket Outer Casing: No cracks were identified from dry powder magnetic particle examination of the socket's outer cone. Finite element analysis shows large structural margins for the outer casing, and robustness to any out-of-tolerance conditions. Dimensions of the socket cone were measured during failure analysis to be within drawing dimensions. Socket joint metrology measurements differed by up to about 0.25 inch based on NASA KSC metrology measurements of the socket and pin dimensions. Variability in final dimensions was expected due to the casting process but considered acceptable based on structural analysis showing robust structural margins.

Wire Brooming: Finite element analysis showed that decreasing brooming quality leads to increased creep rates and, consequently, higher outer wire strains. Poorly broomed sockets are predicted to distribute loads unequally into the critical outer wires, decreasing the overall capability of the design. Therefore, fabrication variability of wire brooming may affect wire stress. Forensic reconstruction of the distribution of wires within the socket was found to be non-uniform (Figure 1), which is logical as the operation is manual, not controlled in uniformity by drawing, and is verified for build quality through inspection prior to spelter pour and proof testing, which the failed Aux M4N socket successfully passed prior to installation. However, wire brooming for this socket was not assessed to be out of family or atypical based on subject matter expertise experience. The likelihood of negative effects from poor fabrication/brooming propagating through the build, proof, and inspection process to in-service was deemed highly unlikely. There are no

known process escapes where a socket of this type passed proof test but subsequently failed due to poor build/brooming quality.

Zinc Spelter: Zinc spelter dimensions conformed to the drawing. Gas bubbles, intermittent porosity, and cracks throughout the bulk zinc were found during the forensic analysis, but as discussed earlier, the high outer wire stresses predicted by the FE analysis were not sensitive to these defects. Measured zinc mechanical properties varied significantly, although some of this can be attributed to size effects of the samples excised from the socket; however, there was a large amount of zinc grain anisotropy that, although expected due to the casting process, can create significant variability in mechanical properties based on grain size and orientation. However, as explained, FE analysis predicted negative margins of the outer wires regardless of the zinc material properties selected.
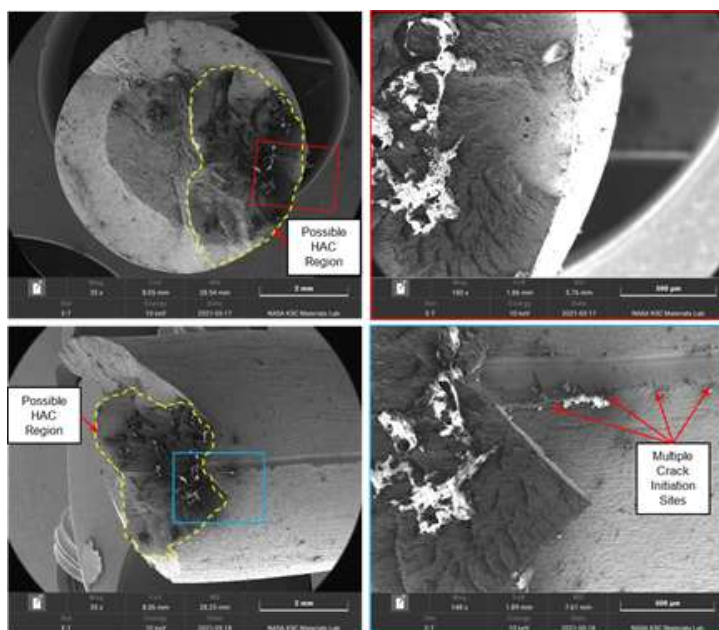

Figure 7. SEM images of surface defect found on a wire.

Poor Wire-Zinc Bond Strength: Fifty-six of the 126 wires fractured in the socket. The other 70 wires did not fracture; the zinc failed before these wires, coming free from the socket attached to most of these wires and the cable-end of the failed wires in a cable/zinc slug. Although 70 wires did not fracture, up to two individual outer ring wires could have pulled free of the socket joint individually due to inadequate wire/zinc bond strength. Of the wires that fractured within the socket and were mechanically removed, some exhibited zinc oxide corrosion product along their wire surfaces down to the wire fracture location, while others exhibited no corrosion with good zinc/metal adhesion along their wire surfaces near the wire fracture location. Consequently, wire-zinc bond strength was not a factor amongst the wire failures and likely not the reason those two wires were found separated from the cable/zinc slug.

Environmental Assisted Degradation

Stress Corrosion Cracking: No evidence of stress corrosion cracking was found during metallurgical studies using visual and SEM inspections. The majority of the wires exhibited a cup-cone ductile failure mode demonstrating that the wires were able to realize their ultimate tensile strengths.

Hydrogen-assisted Cracking (HAC): HAC is caused by diffused hydrogen accumulating at stress concentrations and further decreasing strength capacity of the wires and can lead to wire cracking. Forensic analysis identified three failed wires within the socket that contained evidence of progressive failure, likely HAC. One outer wire had a surface defect at the crack initiation site where the fracture surface exhibited characteristics of HAC (Figure 7). HAC can accelerate failure of a wire, especially when subject to sustained loading with negative structural margins.

Corrosion: The presence of zinc and steel in a humid environment enabled corrosion mechanisms throughout the socket. While some corrosion protective measures were put in service during the life of the socket (e.g., a mastic coating on the casting cap), these measures were put in place after corrosion had begun and were not adequately maintained to provide continued corrosion protection over the life of the socket. This resulted in pervasive quantities of corrosion product, particularly zinc oxide, throughout the socket along various identified moisture pathways. Where steel and zinc were present, heavy amounts of zinc oxide were present with trace amounts of iron oxide. This imbalance in corrosion product is largely due to the cathodic protection of the steel created by the zinc acting as a sacrificial anode in the galvanic corrosion process. The corrosion, while pervasive, was mostly limited to the upper two-thirds of the socket, nearest the casting cap. Of the wires that fractured within the socket and were mechanically removed, some exhibited zinc oxide corrosion product along their wire surfaces down to the wire fracture location, while others exhibited no corrosion, with good zinc/metal adhesion along their wire surfaces near the wire fracture location. Because of this, the forensic evaluation concluded that corrosion played a minimal role in the ultimate failure of the socket.

A finite element study indicated minimal effects on the wire stresses based on a sensitivity study of varying conditions between the socket housing and the zinc. The large compression zone that develops at this interface causes a small sensitivity of the surface conditions on the wire stresses. Analysis evaluated voids within the casting and defects near the casting cap side of the socket and found negligible effects on the maximum predicted wire stress located toward the socket base. This finding was used to assess that corroded wires protruding from the zinc outer diameter were not a factor to the progression of failure. While corrosion was found throughout the zinc, analysis showed a larger role of wire negative margins at operational loads and sustained loading due to deadloads, compared to corrosion in the zinc.

Failure Mechanisms

Strength: Of the 56 wires that failed, five were observed to have surface defects running along their lengths. Two of those defects likely influenced the fracture, and one was an initiation site for a progressive failure, probably HAC, on an outer ring wire. The shear and HAC fractured wires exhibited little to no necking. Outer ring wires that failed typically had less necking than the inner ring wires that failed.

The highest stresses were not predicted to be planar from wire to wire, rather the failure surface followed the surface of a rough spheroid, matching the stepped pattern of wire fracture locations within the socket seen from forensic examination (Figure 8). The outer wires were predicted to fail closer to the socket base cable outlet region, while the inner wires failed slightly inboard to the socket, as seen in the forensic evidence. The stress field suggested that the wires failed adjacent to the greatest confining pressure within the zinc. The zinc plastic flow and the shape of the socket create a region of confining pressure in the shape

of a half spheroid, which causes the highest wire stresses adjacent to the boundary of the highest confining pressure. The red output, showing interface contact pressure ("CPRESS") in Figure 8, reflects the area of highest confining pressure at the zinc/wire interface, which would squeeze the individual wires and suggest the fracture location to be ahead of this region. Regions of colored stars show the different "steps" of failure in the socket. Note that the yellow shading in the top left figure in Figure 8 and the red high stress zones in the lower left figure match the shape of the failure surfaces in the right figure. Model predictions were qualitatively consistent with the observed wire failure modes from the Aux M4N socket. Forensics identified that most wires failed in cup-cone fracture, although a select number of outer wires failed in shear. Analysis shows that the inner wires are under significant confining pressure, thus increasing elongation capability and resulting in a "ductile" cup-cone failure mode.

Figure 8: Highest stresses were not predicted to be planar; failure surface followed a spheroid shape, matching stepped patterns seen in forensic evidence.

In summary, (1) failure in the outer wires occurred prior to zinc core pullout and total cable collapse, (2) the outer wires were critical in maintaining function of the socket joint, and (3) outer wires were highly stressed with minimal structural margins of safety at nominal observatory loads.

Cumulative Damage: Creep was found to be a major contributor to the failure for the following reasons: (1) Forensic analysis showed clear evidence of creep within the zinc (Figure 9). Zinc microstructure nearest the cable/zinc boundary was fully recrystallized with a predominance of grain boundaries aligned 45° to the shear stress, as expected for creep in pure zinc at ambient temperatures. The zinc nearest the socket base, adjacent to the cable/zinc boundary, was determined to be in the late secondary or tertiary stage of creep. Small, non-connected cracks are present within the fully recrystallized grain region near the cable/zinc boundary (Figure 9), running parallel with the cable-end section. These cracks are either from the tertiary stage or cavitation/voids that were squeezed closed due to continued confining pressure imposed by the cable tension and socket wall. High-magnification image of non-connected cracks in different illuminations after tint etching showed predominantly intergranular cracks, which are associated with slower creep mechanisms. Zinc microstructure nearest the socket casing was partially recrystallized with evidence of highly strained zinc (e.g., twinning / slip bands). (2) Loads analysis also supports a higher percentage of deadloads compared to transient loads. (3) Finite element analysis predicted high stresses within the zinc caused by sustained loading, and as the zinc creeped the outer wire stresses were predicted to increase. The negative structural margins further deteriorated over time due to the creep setting within the zinc, until wire and zinc failure occurred.

Figure 9:. Intergranular cracks present adjacent to cable/zinc slug boundary as seen in brightfield, dark field, and cross-polarized illumination. Klemm's 1 Reagent tint etch at 500X magnification.

Forensic investigation of the examined failed wire surfaces found no evidence of fatigue striations, beach marks, or pearlitic steel fracture surfaces that resemble fatigue fracture even without beach marks or striations. Fatigue striations are correlated to crack advancement per loading cycle, while macroscopic beach marks generally represent some changes in the fatigue loading conditions. Forensic inspection found no evidence of fatigue within the zinc, but minor cyclic loading damage that may not be discernable from creep damage within the zinc casting due to sustained loading. Due to the high outer wire stresses, FE analysis could not rule out damage accumulation due to cyclic loading caused by transient events. Creep failure can be accelerated by minor contributions from cyclic damage.

CONCLUSIONS

Forensic and structural analyses were conducted to determine the cause for the first cable failure Aux M4N of the Arecibo Observatory. Analyses were also supported by materials testing and literature review. It is concluded that the socket joint failure in August 2020 was due to insufficient design criteria that did not explicitly consider socket constituent stress margins or time-dependent damage mechanisms. The socket attachment design was found to have an initially low structural margin and finite life, notably in the outer socket wires, which degraded primarily due to long-term zinc creep effects that were activated by long-term sustained loading and exacerbated by cyclic loading. Additionally, HAC and wire defects were found in a few outer wires that may also have contributed to initial outer wire failures. Design did not explicitly consider the time-dependent effects of creep and cyclic loading on design capability, nor explicitly set service life inspection intervals with pass/fail inspection criteria. It also did not specify an end-of-life capability requirement associated with service life degradation. Verification did not account for a worst-case build condition that was traceable to in-service inspection of features (e.g., zinc creep/extrusion). In-service inspections showed evidence of progressive zinc extrusion on several Arecibo sockets, which in hindsight were evidence of cumulative damage and in effect a missed opportunity to prevent cable failure.

INDUSTRY RECOMMENDATIONS

1. Socket joint constituents should be verified to have positive structural margins for strength, fatigue, and creep failure modes for the service life of the socket for all design load combinations.

2. Periodic visual inspection of socket joints should include pass/fail criteria for zinc extrusion tied to a structural qualification test program that verifies the creep failure mode.

3. Qualified processes such as cable replacement and socket joint refurbishment should then be defined to restore joint capacity in the event of failed inspection.

4. ASCE 19-10 and 19-96 codes should be revisited to ensure that design factors consider time-dependent creep in deadload dominated structures, environmental conditions, and workmanship sensitivity to wire defects or brooming.

ACKNOWLEDGMENTS

REFERENCES

1. Morales, J. C., and Suárez-Colche, L. E., "Collapse of The Arecibo Observatory in Puerto Rico: Reflections from a Structural Engineering Perspective," Revista Internacional de Desastres Naturales, Accidentes e Infraestructura Civil. Vol. 19-20 (1).

2. "Wirerope Works, Inc.," URL: http://www.wireropeworks.com.

3. Harrigan, G. J., Valinia, A., Trepal, N., Goyal, V., Babuska, P. "Arecibo Observatory Auxiliary M4N Socket Termination Failure Investigation," NASA/TM−20210017934 and NESC-RP-20-01585, June 2021.

4. "Auxiliary Main Cable Socket Failure Investigation," Wiss, Janney, Elstner Associates, Inc., WJE No. 2020.5191, June 2021.

5. "Structural Applications of Steel Cables for Buildings," ASCE 19-96, 1996 Edition, 1996.

6. "Standard Guidelines for the Structural Applications of Steel Cables for Buildings," ASCE 19-10, 2010 Edition, 2010.

7. Ali, K., Katsuchi, H., and Yamada, H., "Comparative Study on Structural Redundancy of Cable-Stayed and Extradosed Bridges through Safety Assessment of Their Stay Cables," Engineering, Volume 7, Issue 1, January 2021, pp. 111-123.

Commented [T2 Center2]: Eliminar la numeración de las referencias.

AUTHORS BIOSKETCH

G. Harrigan

*H*as over 20 years of experience in the aerospace industry, currently serving as Associate Principal Engineer with the NASA Engineering & Safety Center. He leads multi-disciplined engineering assessments of structures and fluids systems with expertise in failure investigations. Previously, he worked for both NASA and Industry in the areas of mechanical engineering, structural dynamics, and systems engineering. He has a Bachelor of Science in Mechanical Engineering from Carnegie Mellon University, and Master of Science degrees in Engineering from the Florida Institute of Technology.

V. Goyal

*P*rincipal Engineer at the Aerospace Corporation, adjunct professor at University of California Los Angeles and part-time faculty at the University of Southern California in the Mechanical/Aerospace Engineering Departments. He published several books in the areas of aerospace structures, finite element analysis, and computational methods in engineering. Dr. Goyal is responsible for ensuring the technical integrity, and leadership of technical risk assessments, and leads launch vehicle reuse certification ensuring consistent application and adjudication of technical risk assessments across launch vehicles. He serves in NASA NESC technical teams, has co-authored half-dozen standards, and has over 50+ publications. He holds a B.S. degree in Mechanical Engineering from University of Puerto Rico and a Ph.D. degree in Aerospace Engineering from Virginia Tech.

P. Babuska

*A*t the Aerospace Corporation, Mr. Babuska performs independent structural analysis, requirements verification, failure and anomaly resolution, test program development, and general consulting on numerous launch vehicle and spacecraft programs for the US Space Force, DoD, NASA, and commercial customers. Prior to Aerospace, Mr. Babuska worked at the Air Force Research Laboratory in Albuquerque and completed his MS in Civil Engineering from the University of Washington in Seattle where his primary research focus was on novel applications of high-strain and bend-twist coupled composites.

N. Trepal

*S*enior materials engineer at NASA's Kennedy Space Center where he supports NASA's Commercial Crew, Exploration Ground Systems, and Launch Services Programs with various nondestructive examination and welding related engineering issues. Prior to joining NASA, he was the lead for the Nondestructive Inspection Team at the U.S. Navy's Fleet Readiness Center Southwest and, prior to that, the lead for the Nondestructive Examination Group at the Naval Surface Warfare Center Carderock Division. He received a Bachelor of Science in Materials Science & Engineering from the Georgia Institute of Technology in 2002. His expertise in the field of materials science lies in nondestructive examination of metallic and composite materials, metallurgical failure analysis, and welding and allied processes.